Table I. Porphyrin Core Coordination Parameters (Å) of Five-Coordinate Ferric Porphyrins[a]

complex	Fe-N	Ct···N	Fe···CT	ref
Fe(TPP)I	2.066 (11)	2.014	0.53	19
Fe(TPP)($OClO_3$)	2.001 (5)	1.981	0.30	4
Fe(TPP)($FSbF_5$)	1.978 (3)	1.974	0.15	3
Fe(TPP)($B_{11}CH_{12}$)	1.961 (5)	1.955	0.10	this work

[a] Ct = center of the mean plane of the 24-atom porphyrin core; N = porphinato nitrogen atom (average of four values).

this species is very sensitive to traces of moisture (or other ligands) in both the solid state and solution. It crystallizes from toluene as a monosolvate.[14]

The molecular stereochemistry and bond parameters of the coordination group of Fe(TPP)($B_{11}CH_{12}$)·C_7H_8 are displayed in Figure 1. Interestingly, the carborane anion coordinates to the iron through an unsupported Fe-H-B bridge bond. As we have noted elsewhere,[9] this is a rare form of M-H-B interaction, particularly for large boron clusters.[15] There is no significant distortion of the cage atoms relative to an uncoordinated carborane anion.[16] The coordinated B-H bond (1.25 (4) Å) is ca. 0.2 Å longer than the average of the 10 other B-H bonds. The Fe-H distance is found to be 1.82 (4) Å but the uncertainty in this number may be greater than is implied by the formal error owing to the inherent problems of using X-ray data to position a hydrogen atom in a three-center two-electron bond.[17] Nevertheless, it is longer than the corresponding distances found in ferraboranes with Fe-H-B interactions.[18] This is consistent with a higher oxidation state of iron and weak coordination of the carborane anion.

The coordination of a B-H bond makes it difficult to evaluate the metal-anion bond length as a criterion of interaction strength. However, the iron-porphyrin bond parameters are an unusually sensitive guide to the nature of the interaction with the anion and they indicate an extremely weak interaction. Table I compares the core coordination parameters of a series of isostructural complexes where X = I^-, ClO_4^-, SbF_6^-, and $B_{11}CH_{12}^-$. Fe(TPP)I is representative of high-spin five-coordinate ferric porphyrins[12] and has a long average Fe-N bond length (2.066 (11) Å) and a large out-of-plane iron displacement (0.53 Å).[19] These parameters decrease along the series with Fe(TPP)($B_{11}CH_{12}$) having the shortest average Fe-N bond (1.961 (5) Å) and the smallest iron atom displacement (0.10 Å) of any known five-coordinate ferric porphyrin complex. The central hole size of the porphyrin (Ct--N) also follows the same trend.

The core parameters of Table I are the results of two properties of the coordinating anion, its binding strength, and its ligand field strength. Both effects can work in concert thereby amplifying the changes observed along the series. The binding strength is the usual combination of electronic and steric effects that control bond formation. The ligand field effect has been discussed at length: the weaker the axial ligand field, the lower the population of the $d_{x^2-y^2}$ orbital.[4] The gradual lowering of the spin multiplicity is accompanied by a contraction of the coordination core.[20] The end position of the carborane anion in the series must result from it being the weakest binding anion. We note that the carborane anion cannot engage in $p\pi$ donation, a factor that could give rise to weak field characteristics despite strong binding. Since O and F atom ligands may act as $p\pi$ donors their weak field character must not necessarily be taken to indicate weak binding. The carborane anion is clearly the weakest σ-donor in the series.

In summary, the core coordination parameters of five-coordinate M(III) metalloporphyrins appear to provide a generally useful structural criterion for the strength of anion binding. The present results lead to the suggestion that $B_{11}CH_{12}^-$ is the least coordinating anion known to date, at least for the $[Fe(TPP)]^+$ moiety. We are currently extending these studies to other coordinatively unsaturated cations and to related carborane anions of even lower coordinating potential.

Acknowledgment. This work was supported at the University of Southern California by the National Science Foundation (Grant CHE-8519913) and at the University of Notre Dame by the National Institutes of Health (Grant HL-15627).

Supplementary Material Available: Tables of fractional atomic coordinates, anisotropic thermal parameters, and isotropic thermal parameters for the hydrogen atoms (5 pages). Ordering information is given on any current masthead page.

(14) Crystal data: Fe($N_4C_{44}H_{28}$)($B_{11}CH_{12}$)·C_7H_8: triclinic, a = 13.660 (2) Å, b = 14.656 (3) Å, c = 13.142 (2) Å, α = 94.85 (1)°, β = 109.63 (1)°, γ = 75.81 (1)°; space group $P\bar{1}$; z = 2; ρ_{calcd} = 1.25, ρ_{obsd} = 1.24 g/cm^3; R_1 = 0.079, R_2 = 0.092; 7446 unique observed data ($F_o > 3\sigma(F_o)$, $2\theta < 54.9°$). Intensity data were collected at 293 K on a Nicolet P$\bar{1}$ diffractometer with graphite monochromated Mo Kα radiation (λ = 0.71073 Å) using θ-2θ scanning.

(15) (a) Grimes, R. N. In *Metal Interactions with Boron Clusters*; Grimes, R. N., Ed.; Plenum Press: New York, 1982; Chapter 7. (b) Teller, R. G.; Bau, R. *Struct. Bonding (Berlin)* **1981**, *44*, 1.

(16) In comparison to [Fe(TPP)(THF)][$B_{11}CH_{12}$]; complete details of this and the present structure will be published: Shelly, K.; Lee, Y. J.; Scheidt, W. R.; Reed, C. A., manuscript in preparation.

(17) (a) Takusagawa, F.; Fumagalli, A.; Koetzle, T.; Shore, S. G.; Schmitkons, T.; Fratini, A. V.; Morse, K. W.; CWei, C.-Y.; Bau, R. *J. Am. Chem. Soc.* **1981**, *103*, 5165. (b) Beno, M. A.; Williams, J. M.; Tachikawa, M.; Muetterties, E. L. *Ibid.* **1981**, *103*, 1485.

(18) Fe-H distances range from 1.56 to 1.61 Å; see: (a) Fehlner, T. P.; Housecroft, C. E.; Scheidt, W. R.; Wong, K. S. *Organometallics* **1983**, *2*, 825. (b) Haller, K. J.; Anderson, E. L.; Fehlner, T. P. *Inorg. Chem.* **1981**, *20*, 309. (c) Mangion, M.; Ragaini, J. D.; Schnitkons, T. A.; Shore, S. G. *J. Am. Chem. Soc.* **1979**, *101*, 754.

(19) Hatano, K.; Scheidt, W. R. *Inorg. Chem.* **1979**, *18*, 877.

(20) Along the series X = I^-, ClO_4^-, SbF_6^-, $B_{11}CH_{12}^-$ the spin state changes from $S = {}^5/_2$ ($d_{x^2-y^2}$ populated), through admixed $S = {}^3/_2$, ${}^5/_2$ to essentially pure $S = {}^3/_2$ ($d_{x^2-y^2}$ unpopulated). Both the SbF_6^- and $B_{11}CH_{12}^-$ complexes have nearly identical magnetic and Mössbauer characteristics that are indicative of an essentially pure $S = {}^3/_2$ spin state.

Microporous Aluminum Oxide Films at Electrodes. 3. Lateral Electron Transport in Self-Assembled Monolayers of *N*-Methyl-*N'*-octadecyl-4,4'-bipyridinium Chloride

Cary J. Miller and Marcin Majda*

Department of Chemistry, University of California Berkeley, California 94720

Received December 23, 1985

Widespread interest in organized, synthetic monolayers is largely due to their resemblance to biological membranes.[1] They can also be used as subcomponents of multilayer, molecularly organized microstructures.[2] We report here on the direct electrochemical measurement of the lateral electron transport in a monolayer assembly of electroactive amphiphilic molecules. Porous aluminum oxide films at gold electrodes[3] were used as substrates for self-organization of the assembly.

Assembly of amphiphilic monolayers can be accomplished by well-developed Langmuir-Blodgett techniques[4] and by the molecular self-organization process.[5] Both methods are capable of producing films equivalent in structure and in the degree of molecular organization.[5,6a-c] As demonstrated recently by Sagiv, adsorption and self-assembly of alkyltrichlorosilanes on polar surfaces lead, in addition, to the formation of chemically bonded monolayers of remarkable stability.[6b,7a-c] Also, molecular self-

(1) Fendler, J. H. *Membrane Mimetic Chemistry*; Wiley: New York, 1982.

(2) See for example: Kuhn, H. *Thin Solid Films* **1983**, *99*, 1.

(3) (a) Miller, C. J.; Majda, M. *J. Am. Chem. Soc.* **1985**, *107*, 1419. (b) Miller, C. J.; Majda, M. *J. Electroanal. Chem.*, in press.

(4) Kuhn, H.; Möbius, D.; Bücher, H. In *Physical Methods of Chemistry*, Weissberger, A.; Rossiter, B. W., Eds.; Wiley: New York, 1972; Vol. 1, Part III, p 577.

(5) Allara, D. L.; Nuzzo, R. G. *Langmuir* **1985**, *1*, 45 and references therein.

(6) (a) Allara, D. L.; Nuzzo, R. G. *Langmuir* **1985**, *1*, 52. (b) Maoz, R.; Sagiv, J. *J. Colloid Interface Sci.* **1984**, *100*, 465. (c) Gun, J.; Iscovici, R.; Sagiv, J. *J. Colloid Interface Sci.* **1984**, *101*, 201.

0002-7863/86/1508-3118$01.50/0

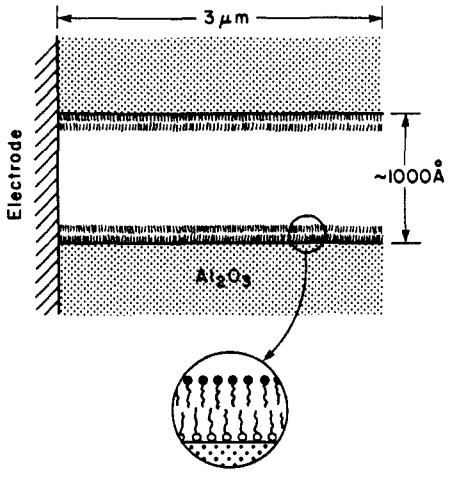

Figure 1. Schematic cross section of a single pore of a porous aluminum oxide film at a gold electrode with the self-assembled bilayer composed of *n*-octadecyltrichlorosilane (surfactant molecules marked with open circles) and *N*-methyl-*N'*-octadecyl-4,4'-bipyridinium chloride (surfactant molecules marked with closed circles).

organization of monolayers takes place on surfaces regardless of the shape and the level of dispersion of the substrate, and, therefore, is not restricted to large flat substrates typically used in Langmuir–Blodgett transfer experiments.

Relying on the molecular self-organization process, we have produced a stable, bilayer-like assembly of two different amphiphilic molecules on the surface of aluminum oxide. The bilayer consists of a monomolecular layer of *n*-octadecyltrichlorosilane (OTS) self-assembled in the first step of the preparation scheme on the aluminum oxide surface. Following this step, a layer of *N*-methyl-*N'*-octadecylviologen ($C_{18}MV^{2+}$) self-assembles upon exposure of the hydrophobic OTS surface to a dilute aqueous solution of $C_{18}MV^{2+}$. The aluminum oxide substrate used in these experiments is a 3-μm-thick microporous alumina layer deposited at a gold electrode. We have recently described the preparation and properties of such porous aluminum oxide films at electrodes as support matrices for immobilization of electroactive reagents.[3] The most distinct feature of these films is their geometrically regular porosity which consists of a dense array of cylindrical pores propagating through the entire thickness of the oxide film normal to its surface. The inner surfaces of these pores, whose diameter is approximately 1000 Å, are coated with the bilayer assembly mentioned above. A schematic drawing of an individual pore of the oxide film at the electrode surface and the idealized structure of the bilayer are shown in Figure 1. We report below our preliminary results which allowed us to postulate the formation and the structure of the bilayer assembly illustrated in Figure 1.

The porous oxide films used in this work were produced electrochemically at 65 V in 4% H_3PO_4 and treated as described previously.[3b] The adsorption and self-organization of an OTS monolayer on the oxide surfaces was accomplished by exposing a dry 3-μm-thick section of the aluminum oxide to a 0.5% solution of OTS in hexadecane for 15 min.[6b] Afterward, the oxide film was rinsed sequentially with an excess of hexadecane, toluene, and isopropyl alcohol. Its surface was hydrophobic, exhibiting a contact angle of over 100° with water. The OTS-treated sections of the oxide are then overcoated with gold and fabricated into electrodes.[3b] Upon exposure of these electrodes to a dilute (0.05–0.2 mM) solution of $C_{18}MV^{2+}$ chloride,[8] one observed incorporation of $C_{18}MV^{2+}$ into the OTS-treated oxide films as evidenced by a growth of the voltammetric waves due to redox activity of the viologen centers. The steady-state level of incorporation (attainable in a stirred solution in approximately 10 min) is 2×10^{-10} mol/cm^2 of the internal geometric surface area of the oxide film. This corresponds to a monomolecular coverage of $C_{18}MV^{2+}$ molecules. The immobilization of $C_{18}MV^{2+}$ molecules within the OTS oxide film is remarkably stable in that no significant loss of electroactivity was observed after 30 min of potential cycling in a 0.1 M KCl solution free of $C_{18}MV^{2+}$. All the following electrochemical experiments described here were done in electrolyte solutions that did not contain any deliberately added octadecylviologen.

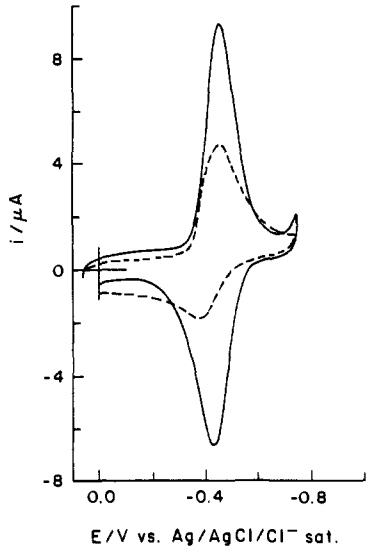

Figure 2. Steady-state cyclic voltammograms of *N*-methyl-*N'*-octadecyl-4,4'-bipyridinium chloride self-assembled at a 3-μm-thick (average pore diameter 1000 Å), OTS-treated, porous aluminum oxide film at an Au electrode.[3] Dashed line, 0.1 M KCl, v = 20 mV/s; continuous line, the same electrode transferred to 0.1 M KCl, 3 mM 1-octanol, v = 20 mV/s. The smaller charge under the dashed line voltammogram (pure KCl electrolyte) compared to the charge under the continuous line voltammogram (KCl + 1-octanol electrolyte) reflects the partial loss of electroactivity of the system under continuous voltammetric cycling in the absence of 1-octanol (see text).

If the bilayer structure shown in Figure 1 reflects indeed the true nature of the system, the porosity of the oxide film after the assembly process should not be substantially different from the porosity of the underivatized film since the average pore diameter of 1000 Å is much larger than the thickness of the bilayer. Porosity measurements were obtained by rotating disk voltammetry with *p*-benzoquinone as an electroactive probe followed by the Koutecky–Levich data analysis.[3b,9] The relative porosity values obtained for the untreated Al_2O_3 film at a gold electrode, OTS–Al_2O_3 film, and $C_{18}MV^{2+}$–OTS–Al_2O_3 film were 51%, 44%, and 41% (all ±3%), respectively, in support of the structure in Figure 1.

As shown in Figure 2 (dashed line), the voltammetric reduction of $C_{18}MV^{2+}$ in the bilayer assembly results in a partial loss of electroactivity due, most likely, to the dimerization of the viologen cation radical species and the formation of hydrophobic, electroinactive aggregates. The equilibration of the system at a positive potential restores the original level of electroactivity. A remarkable improvement of the voltammetric reversibility of the system was observed upon addition of 3 mM 1-octanol to the 0.1 M KCl supporting electrolyte (see Figure 2, continuous line). The total quantity of the assembled $C_{18}MV^{2+}$ does not change but the reduction and the oxidation processes become fully reversible. The sharper voltammetric peaks suggest also a faster rate of charge transport along the bilayer. The chronocoulometric measurements of the rate of charge propagation showed typically a 6-fold increase in the apparent diffusion coefficient upon octanol addition. (D_{app} = 4×10^{-8} cm^2/s and 2×10^{-7} cm^2/s were measured before and after the addition of octanol to the electrolyte solution.) 1-Hexanol

(7) (a) Sagiv, J. *J. Am. Chem. Soc.* **1980**, *102*, 92. (b) Netzer, L.; Sagiv, J. *J. Am. Chem. Soc.* **1983**, *105*, 647. (c) Netzer, L.; Iscovici, R.; Sagiv, J. *Thin Solid Films* **1983**, *99*, 235; **1983**, *100*, 67.

(8) Critical micelle concentration of $C_{18}MV^{2+}$ is 1.4×10^{-3} M: Brugger, P. A.; Infelta, P. P.; Braun, A. M.; Grätzel, M. *J. Am. Chem. Soc.* **1981**, *103*, 320.

(9) Gough, D. A.; Leypoldt, J. K. *Anal. Chem.* **1979**, *51*, 439.

and 1-decanol have similar effects on the behavior of the system when present in the supporting electrolyte. The influence of the aliphatic alcohols is reversible and persists only during their presence in the bulk of the electrolyte solution.

It seems reasonable to explain these observations by postulating that the alcohol molecules associate with the octadecylviologen layer, likely through intercalation of their hydrocarbon tails into the $C_{18}MV^{2+}$ layer. This then leads to a drastic change of solvation environment around the bipyridyl groups and prevents the formation of electroinactive dimers and/or aggregates. The dimerization of methylviologen cation radical has been known to occur in aqueous solutions and does not take place in media of low polarity.[10] Recently the equilibrium constant for the dimerization of $MV^{\bullet+}$ was observed by Kaifer and Bard to decrease in the presence of anionic micelles and was interpreted to indicate that $MV^{\bullet+}$ species reside in a hydrophobic environment of the micelles' core.[11] The increase of the apparent diffusion coefficient reported above is related to an increase of the fluidity of the $C_{18}MV^{2+}$ monolayer intercalated with alcohol molecules.

The results of the electrochemical experiments reported here constitute, to our best knowledge, the first direct measurements of the lateral electron transport in organized monolayers. These measurements were possible primarily because of the unique geometry of the pore structure of the aluminum oxide films used as substrates.[3a,b] Many intriguing questions related to the dynamics of the electron propagation in self-assembled layers as a function of their composition and the type of intercalating agents are currently under investigation.

Acknowledgment. We gratefully acknowledge the support of the National Science Foundation (CHE-8504368).

(10) Kosower, E. M.; Cotter, J. L. *J. Am. Chem. Soc.* **1964**, *86*, 5524.
(11) Kaifer, A. E.; Bard, A. J. *J. Phys. Chem.* **1985**, *89*, 4876.

Structural Diversity of F_{430} from *Methanobacterium thermoautotrophicum*. A Nickel X-ray Absorption Spectroscopic Study

Marly K. Eidsness,[†,1a] Richard J. Sullivan,[1b] James R. Schwartz,[1b] Patricia L. Hartzell,[1c] Ralph S. Wolfe,[1c] Anne-Marie Flank,[1d] Stephen P. Cramer,[1e] and Robert A. Scott*[1b]

Department of Microbiology and School of Chemical Sciences, University of Illinois, Urbana, Illinois 61801
Department of Materials Science, Stanford, University Stanford, California 94305
LURE, Batîment 209C, 91405 Orsay, France
Exxon Research and Engineering Annandale, New Jersey 08801

Received December 23, 1985

Nickel metalloenzymes have been found in all methane-producing bacteria examined.[2] Two hydrogenases from *Methanobacterium thermoautotrophicum* contain nickel,[3-5] which has been shown to be coordinated by S-containing ligands in one form.[5]

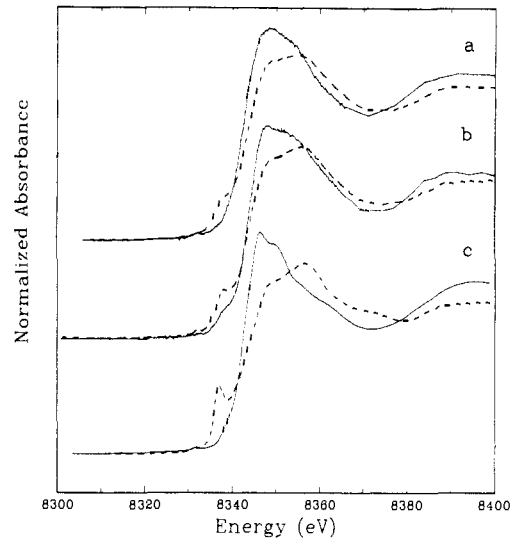

Figure 1. Nickel K absorption edge spectra for various forms of F_{430} from *M. thermoautotrophicum* compared with model compounds: (a) intact component C (solid line) and free F_{430} (dashed line), (b) salt-extracted F_{430} (solid line) and heat-extracted F_{430} (dashed line), and (c) six-coordinate $[Ni(en)_3]^{2+}$ (solid line) and four-coordinate square-planar Ni(ibc) (dashed line). The preedge feature at 8336 eV is a signature for Ni four-coordinate square-planar geometry (see text).

A very similar Ni-containing hydrogenase occurs in *Desulfovibrio gigas*.[6] A compound called F_{430} has been isolated from *M. thermoautotrophicum*, strain ΔH,[7] and has been identified as the Ni-containing prosthetic group in protein component C of the *S*-methyl coenzyme-M reductase system.[8,9] This enzyme complex catalyzes the final step in methanogenesis, the two-electron reduction of the methyl group in *S*-methyl coenzyme M [2-(methylthio)ethanesulfonate] to methane:

$$CH_3SCH_2CH_2SO_3^- + 2e^- + 2H^+ \rightarrow CH_4 + HSCH_2CH_2SO_3^-$$

F_{430} has been established to have a Ni(II)-tetrapyrrole structure,[10] constituting the only known biological example of nickel in a tetrahydro reduced corphine. The detailed mechanistic role of F_{430} in methyl group reduction has not been identified.

We report here a Ni X-ray absorption spectroscopic (XAS) study of several forms of F_{430} and component C isolated from *M. thermoautotrophicum*, strain ΔH. These preliminary results indicate that "free" F_{430}[11] is structurally distinct from the F_{430}-containing protein. Also, depending upon the conditions used, extraction of F_{430} from the protein yields at least two structurally distinct forms, one similar to that in the intact protein and one similar to free F_{430}. Analysis of the extended X-ray absorption fine structure (EXAFS) data and comparison with a number of structurally characterized Ni(II) complexes provide evidence that the flexibility of the tetrapyrrole is responsible for the different structural forms.

M. thermoautotrophicum cell extract was prepared as described previously[12] and component C was prepared from the cell extract following published procedures[13] except that phenyl-Sepharose

[†] Present address: School of Chemical Sciences, University of Illinois.
(1) (a) Stanford University. (b) School of Chemical Sciences, University of Illinois. (c) Department of Microbiology, University of Illinois. (d) LURE. (e) Exxon Research and Engineering.
(2) Diekert, G.; Konheiser, U.; Piechulla, K.; Thauer, R. K. *J. Bacteriol.* **1981**, *148*, 459-464.
(3) Jackson, F. S.; Daniels, L.; Fox, J. A.; Walsh, C. T.; Orme-Johnson, W. H. *J. Biol. Chem.* **1982**, *257*, 3385-3388.
(4) Kojima, N.; Fox, J. A.; Hausinger, R. P.; Daniels, L.; Orme-Johnson, W. H.; Walsh, C. T. *Proc. Natl. Acad. Sci. U.S.A.* **1983**, *80*, 378-382.
(5) Lindahl, P. A.; Kojima, N.; Hausinger, R. P.; Fox, J. A.; Teo, B.-K.; Walsh, C. T.; Orme-Johnson, W. H. *J. Am. Chem. Soc.* **1984**, *106*, 3062-3064.
(6) Scott, R. A.; Wallin, S. A.; Czechowski, M.; DerVartanian, D. V.; LeGall, J.; Peck, H. D., Jr.; Moura, I. *J. Am. Chem. Soc.* **1984**, *106*, 6864-6865.
(7) Gunsalus, R. P.; Wolfe, R. S. *FEMS Microbiol. Lett.* **1978**, *3*, 191-193.
(8) Ellefson, W. L.; Whitman, W. B.; Wolfe, R. S. *Proc. Natl. Acad. Sci. U.S.A.* **1982**, *79*, 3707-3710.
(9) *S*-Methyl coenzyme-M reductase activity can be reconstituted only by inclusion of other protein and cofactor components with the purified F_{430}-containing protein on which our studies were performed. This F_{430}-containing protein is referred to as component C.
(10) Pfaltz, A.; Jaun, B.; Fassler, A.; Eschenmoser, A.; Jaenchen, R.; Gilles, H. H.; Diekert, G.; Thauer, R. K. *Helv. Chim. Acta* **1982**, *65*, 828-865.
(11) "Free" F_{430} was purified from the cell extract pool of low molecular weight cofactors not bound to protein.
(12) Gunsalus, R. P.; Wolfe, R. S. *J. Biol. Chem.* **1980**, *255*, 1891-1895.

0002-7863/86/1508-3120$01.50/0